

# *Caenorhabditis elegans* oocytes detect meiotic errors in the absence of canonical end-on kinetochore attachments

Amanda C. Davis-Roca, Christina C. Muscat, and Sarah M. Wignall

Department of Molecular Biosciences, Northwestern University, Evanston, IL 60208

Mitotically dividing cells use a surveillance mechanism, the spindle assembly checkpoint, that monitors the attachment of spindle microtubules to kinetochores as a means of detecting errors. However, end-on kinetochore attachments have not been observed in *Caenorhabditis elegans* oocytes and chromosomes instead associate with lateral microtubule bundles; whether errors can be sensed in this context is not known. Here, we show that *C. elegans* oocytes delay key events in anaphase, including AIR-2/Aurora B relocalization to the microtubules, in response to a variety of meiotic defects, demonstrating that errors can be detected in these cells and revealing a mechanism that regulates anaphase progression. This mechanism does not appear to rely on several components of the spindle assembly checkpoint but does require the kinetochore, as depleting kinetochore components prevents the error-induced anaphase delays. These findings therefore suggest that in this system, kinetochores could be involved in sensing meiotic errors using an unconventional mechanism that does not use canonical end-on attachments.

## Introduction

Proper partitioning of chromosomes during cell division is essential for organismal viability. During mitosis, chromosomes attach to spindle microtubules at sites called kinetochores, forming end-on attachments that mediate chromosome congression and segregation (Cheerambathur and Desai, 2014). These attachments are also central to a surveillance mechanism, the spindle assembly checkpoint (SAC), in which cells monitor the attachment of kinetochores to spindle microtubules as a means of detecting errors (Etemad and Kops, 2016). However, homologous chromosome pairs (bivalents) in *Caenorhabditis elegans* oocytes do not appear to form end-on attachments and instead are surrounded by laterally associated microtubule bundles running along their sides (Wignall and Villeneuve, 2009). Whether these oocytes are able to detect and respond to errors is currently unknown.

*C. elegans* have holocentric kinetochores that, in meiosis, cap the ends of each bivalent (Monen et al., 2005). Compromising kinetochore function by depleting KNL-1 (which is required for the loading of the MIS-12 complex, the RZZ complex, and BUB-1) results in chromosome alignment defects during metaphase (Dumont et al., 2010), suggesting that these holocentric kinetochores help orient bivalents within the lateral microtubule bundles. Despite this, chromosome segregation appears to be largely kinetochore independent, as kinetochores are normally removed from chromosomes during anaphase. Moreover, although KNL-1 depletion results in some lagging

chromosomes, most segregate at normal rates, suggesting that kinetochore attachments are not generating the forces that drive segregation (Dumont et al., 2010).

Instead, chromosome congression and segregation are aided by a protein complex that forms a ring around the center of each bivalent in meiosis I (MI) and around the interface between sister chromatids in MII; we refer to these complexes as midbivalent rings. These rings contain the kinesin-4 family member KLP-19, which has been proposed to provide chromosomes with a plus-end-directed force that promotes movement to the metaphase plate along the laterally associated bundles (Wignall and Villeneuve, 2009). Then, in anaphase, these rings are removed from chromosomes (Dumont et al., 2010), removing this plus-end-directed force and allowing poleward movement (Muscat et al., 2015); additionally, the spindle also significantly elongates during anaphase, driving chromosomes further apart (Dumont et al., 2010; McNally et al., 2016). In addition to KLP-19, the ring complexes include several other conserved cell division proteins (Dumont et al., 2010; Collette et al., 2011; Connolly et al., 2015; Han et al., 2015) and the chromosomal passenger complex (Wignall and Villeneuve, 2009), which consists of AIR-2/Aurora B kinase, ICP-1, CSC-1, and BIR-1 (Schumacher et al., 1998; Speliotes et al., 2000; Romano et al., 2003) and is required for the targeting

Downloaded from <http://rupress.org/journal/jcb/216/5/1243/1604354/jcb-201608042.pdf> by guest on 09 February 2026

Correspondence to Sarah M. Wignall: [s-wignall@northwestern.edu](mailto:s-wignall@northwestern.edu)

Abbreviations used: MI, meiosis I; SAC, spindle assembly checkpoint; SEP-1, separase.



of all other known ring components (Wignall and Villeneuve, 2009; Dumont et al., 2010).

Now, we have discovered that the behavior of these ring complexes changes in anaphase when errors are present. Surprisingly, despite the apparent lack of end-on attachments in this system, this error response requires the kinetochore. Our studies have therefore revealed a new mechanism that appears to regulate the progression of anaphase events in this specialized form of cell division and also suggest that the kinetochore plays a noncanonical role in error detection in these cells.

## Results and discussion

### The presence of univalents alters AIR-2/Aurora B behavior in anaphase

In a previous study, we assessed the contribution of the midbivalent ring complex to chromosome congression and segregation by examining the behavior of univalents, which do not undergo crossover formation and therefore lack rings (Muscat et al., 2015). We used the *him-8* mutant, in which the X chromosomes fail to pair (Phillips et al., 2005), resulting in five ring-containing bivalents that segregate normally and two univalents that exhibit alignment and segregation defects (Muscat et al., 2015). Unexpectedly, during these studies, we noticed unusual ring behavior in the *him-8* mutant during anaphase (Fig. 1).

During wild-type meiosis, separase (SEP-1) moves from the kinetochores to the ring complexes at anaphase onset, and as the chromosomes begin segregating, the rings remain at the center of the spindle (Dumont et al., 2010; Muscat et al., 2015). Shortly after, ring component AIR-2/Aurora B relocates across the spindle (Schumacher et al., 1998) and the ring structures begin disassembling and are gone by late anaphase (Fig. 1 A; Dumont et al., 2010; Muscat et al., 2015). In contrast, in the *him-8* mutant, AIR-2 often associated with the ring complexes in mid to late anaphase, and under these conditions, the rings appeared more intact instead of flattening (Fig. 1 B).

To quantify this behavior, we evaluated 246 wild-type spindles and established a chromosome segregation distance that we defined as the transition from early to mid anaphase, when AIR-2 should no longer be ring associated. From this analysis, we found that AIR-2 had relocalized to microtubules in a majority of wild-type spindles when the chromosomes were  $\geq 2.5 \mu\text{m}$  apart (Fig. S1); at  $\geq 2.5 \mu\text{m}$ , only 8% of mid anaphase spindles had AIR-2 in ring structures. In contrast, using these same criteria, we found that AIR-2 was ring associated (though sometimes faintly relocalized to the microtubules) in 34% of mid anaphase spindles in the *him-8* mutant (Fig. 1 C). We observed similar behavior in the *zim-1* mutant (where chromosomes I and III fail to pair, resulting in four univalents; Phillips and Dernburg, 2006), demonstrating that autosomal univalents also trigger this behavior (Fig. 1, B and C); in both mutants, we observed these changes in both MI and MII (Fig. 1, B and C). Importantly, AIR-2 was never associated with the ring complexes at late anaphase, when the polar body begins to pinch off (Fig. 1 B). Therefore, AIR-2 relocalization is delayed, but not prevented, in the presence of univalents.

### Defects before anaphase onset and environmental stresses can delay ring disassembly

Next, we wanted to determine whether this altered AIR-2 behavior was specific to mutants containing univalents or whether

this behavior would also occur after other types of perturbations, which would be suggestive of a general regulatory mechanism. First, we induced spindle defects either by depleting spindle-pole protein ASPM-1 (van der Voet et al., 2009; Connolly et al., 2014) or by analyzing a partial loss-of-function mutant of the microtubule severing protein, MEI-2/katanin (Srayko et al., 2000; McNally et al., 2006). In both cases, AIR-2 remained in rings in a significant fraction of mid anaphase spindles (Fig. 2, A and D), demonstrating that spindle disorganization can alter AIR-2 behavior. Second, because the midbivalent ring complex has been implicated in chromosome congression and segregation (Wignall and Villeneuve, 2009; Dumont et al., 2010; Muscat et al., 2015), we depleted ring components KLP-19 and CAPG-1, and we observed a similar delay in AIR-2 relocalization (Fig. 2, A, B, D, and E); AIR-2 metaphase localization is unaffected after depletion of these proteins (Dumont et al., 2010; Collette et al., 2011), allowing us to assess anaphase behavior. Therefore, AIR-2 anaphase behavior is altered in response to many types of perturbations.

Some spindles with altered AIR-2 behavior had severely lagging chromosomes (Fig. 2 B), but others did not (Figs. 1 B and 2 A), indicating that this delay can occur in the absence of obvious chromosome segregation defects and is not caused by chromosomes directly contacting the rings. Additionally, under conditions where AIR-2 remained ring associated, other ring proteins were also retained in the structures (Fig. 2 E), and all rings within the spindle behaved similarly, suggesting a global mechanism that leads to general ring stabilization. Our observations are therefore consistent with the idea that AIR-2 relocalizing to the microtubules and ring disassembly are regulated processes that can be delayed in the presence of errors.

To determine whether errors occurring after anaphase onset can also alter AIR-2 and ring behavior, we individually depleted proteins required for cytokinesis: the centalspindlin components ZEN-4 and CYK-4 (Raich et al., 1998; Jantsch-Plunger et al., 2000) and the anillin-related protein, ANI-1 (Maddox et al., 2005). In each case, AIR-2 and ring behavior were indistinguishable from control anaphase spindles in MI (Fig. 2, C and D). This was not caused by ineffective RNAi, as we observed MII spindles with twice the normal number of chromosomes (caused by MI cytokinesis failure), and in many of those anaphase II spindles, AIR-2 remained ring associated (Fig. 2 C). Together, our results suggest that errors occurring before anaphase can alter AIR-2 anaphase behavior, but defects in late anaphase do not trigger a change, likely because at that point, AIR-2 would have already relocalized.

Finally, we investigated whether other types of stresses affect anaphase ring behavior. The standard range of growth temperatures for *C. elegans* is 15–25°C (Brenner, 1974), but worms begin to lose fecundity >24°C (Hirsh et al., 1976). After short exposures to either low (4°C) or high (25°C or 30°C) temperatures, AIR-2 relocalization to microtubules and ring disassembly were delayed (Fig. 2, A and D). Therefore, disassembly of the midbivalent ring is a regulated process that is altered in response to meiotic errors and unfavorable environmental conditions.

### Microtubule channels remain open and kinetochore disassembly is delayed in response to error

When assessing ring behavior in various mutant conditions, we noticed that anaphase spindle morphology often differed from the control (Fig. 1 B and Fig. 2, A, B, and E). Therefore, we

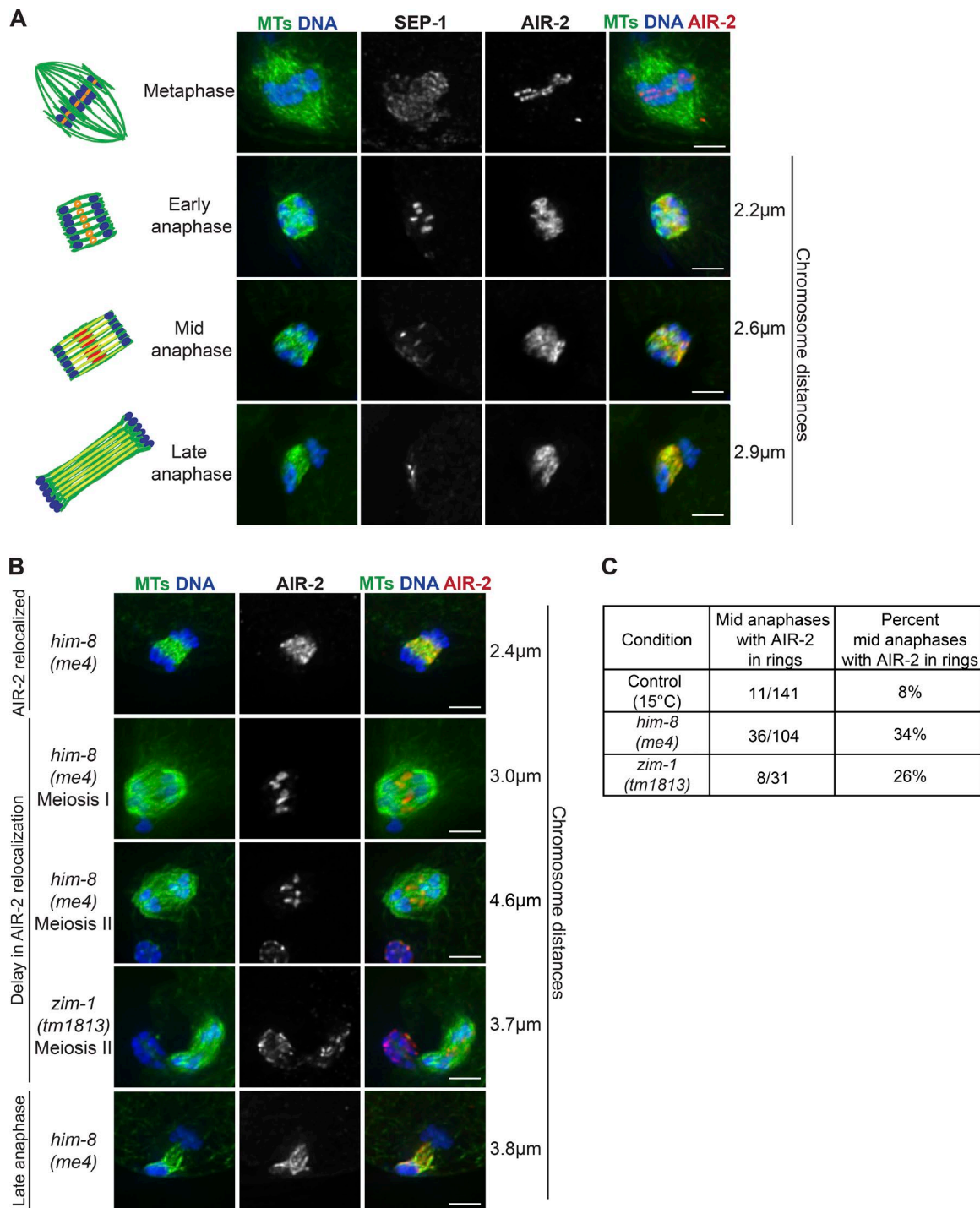


**Figure 1. AIR-2/Aurora B anaphase behavior is altered in the presence of univalents.** (A) Wild-type anaphase spindles stained for DNA (blue), tubulin (green), SEP-1, and AIR-2 (red in merge). The chromosome segregation distances and spindle morphology were used to determine the anaphase stages. Diagrams depict DNA (blue), microtubules (green), AIR-2 (yellow), the rings without AIR-2 (red), and the rings containing AIR-2 (orange). (B) AIR-2 behavior in spindles containing univalents in either the *him-8(me4)* or the *zim-1(tm1813)* mutant. In some spindles, AIR-2 relocates to microtubules by mid anaphase (row 1), whereas in others, AIR-2 remains ring associated in MI (row 2) and MII (rows 3 and 4); note that in MII, AIR-2 also displays polar body localization. AIR-2 always relocates by late anaphase (row 5). (C) Quantification of mid anaphase spindles with AIR-2 in rings for control, *him-8(me4)*, and *zim-1(tm1813)* MI and MII spindles. Bars, 2.5 μm.

decided to compare spindle organization in cases where the rings persisted to those in which rings disassembled normally. In control oocytes, spindle poles broaden in early anaphase, creating microtubule channels that are open from pole to pole; these channels then close as anaphase progresses, reducing the

width of the central region of the spindle (Fig. 1 A). In most of the mutant spindles we examined, the poles still broadened, organizing the microtubules in a parallel array. However, although in wild-type oocytes the channels in the center of the spindle are typically compressing in mid anaphase, the central region

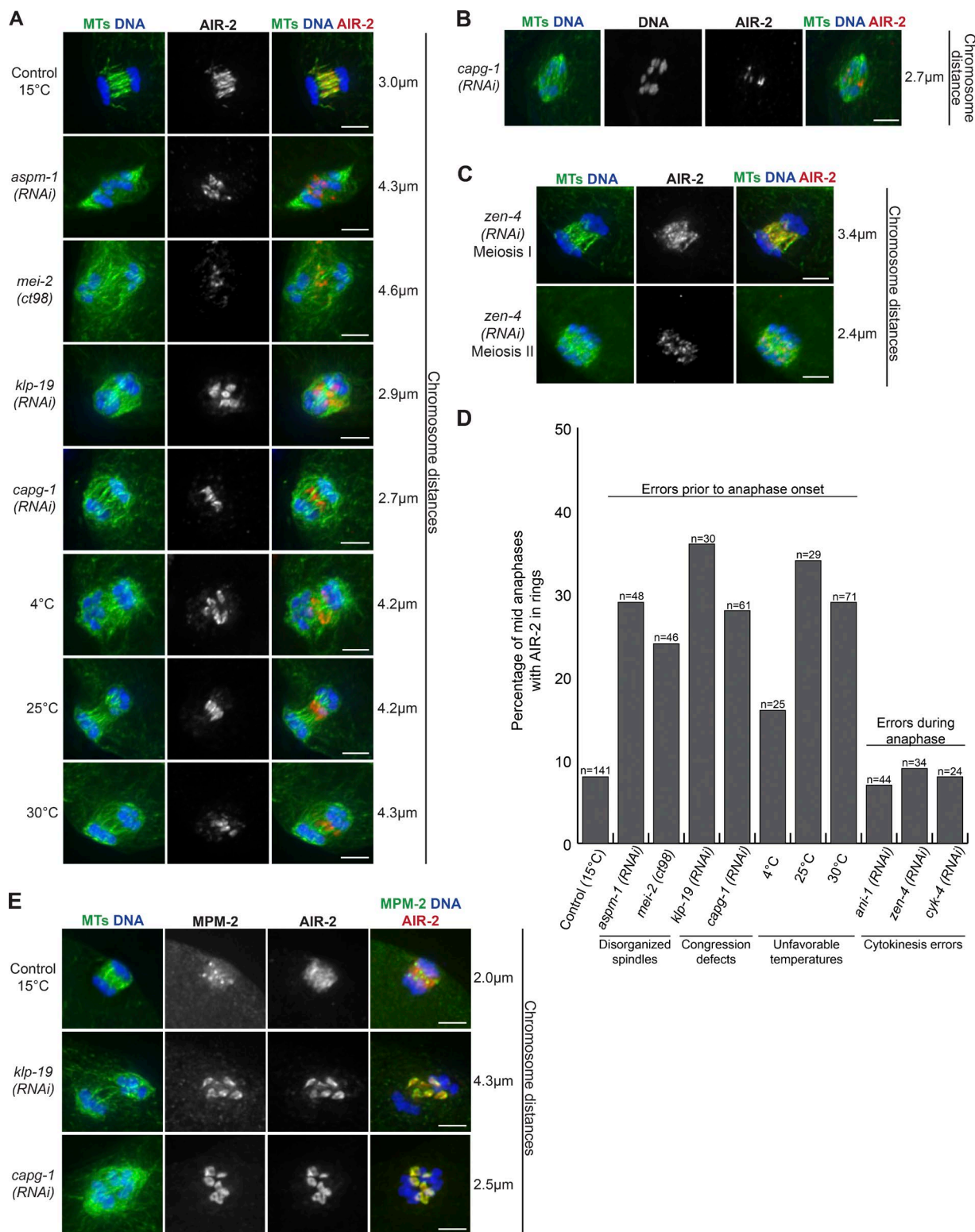


**Figure 2. Defects before anaphase onset and environmental stresses can delay ring disassembly.** (A–C) DNA (blue), tubulin (green), and AIR-2 (red) in control and error-induced spindles. AIR-2 stays ring associated after a variety of perturbations, and ring disassembly is delayed both in spindles with (A) lagging chromosomes. (C) *zen-4*(RNAi) does not delay ring disassembly in MI but can cause AIR-2 to remain in rings in MII when there is double the chromosome number. (D) Quantification of mid anaphase spindles with AIR-2 in rings for all conditions tested and includes MI and MII spindles for all conditions except depletion of *zen-4*, *cyk-4*, and *ani-1*. (E) DNA (blue), tubulin (green, column 1), AIR-2 (red), and MPM-2 (green, column 4) in control and error-induced spindles. MPM-2 marks the ring structures, illustrating that additional ring proteins are stabilized when AIR-2 persists in rings under error conditions. Bars, 2.5 μm.

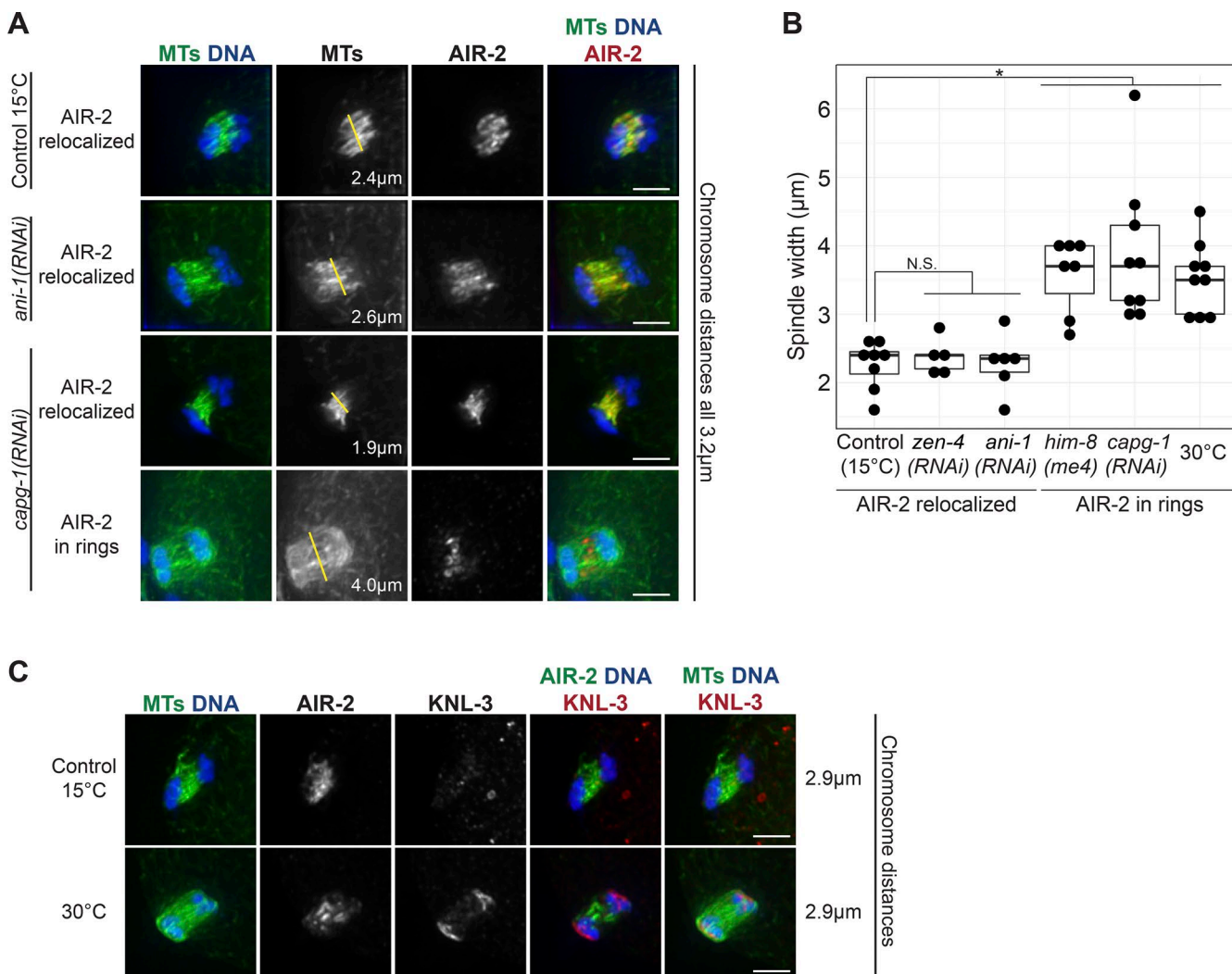


**Figure 3. Microtubule channels remain open and kinetochore disassembly is delayed in response to error.** (A) Spindles stained for DNA (blue), tubulin (green), and AIR-2 (red). When AIR-2 remains in rings (row 4, *capg-1(RNAi)* shown), the spindle is significantly wider than when AIR-2 is microtubule associated (rows 1–3); spindle widths are denoted within each image. (B) Box plot shows the widths of spindles in which AIR-2 is relocalized compared with those in which AIR-2 remains in rings. Spindles measured had chromosome distances between 2.7  $\mu\text{m}$  and 4.2  $\mu\text{m}$ . Box represents first quartile, median, and third quartile. Lines extend to data points within 1.5 interquartile range. N.S., not significant; asterisk represents significant difference (two-tailed *t* test;  $^*, P < 0.001$ ). (C) Spindles stained for DNA (blue), tubulin (green, columns 1 and 5), AIR-2 (green, column 4) and KNL-3 (red). KNL-3 remains chromosome-associated when AIR-2 remains in rings; 30°C treatment shown. Bars, 2.5  $\mu\text{m}$ .

of the spindles often appeared wide in the mutant conditions (Fig. 1 B; Fig. 2, A, B, and E; and Fig. 3 A). We quantified this effect and found that when AIR-2 remained with the ring complexes, spindles were significantly wider than when rings disassembled normally (Fig. 3 B). Moreover, we observed open microtubule channels in the center of the spindle under these conditions (Videos 1 and 2), suggesting that the persistence of rings maintains this microtubule organization.

Another unusual feature we observed in spindles with delayed ring disassembly was increased microtubule density at the poleward surfaces of separating chromosomes. In contrast to control spindles, where the chromosomes move past the poles during mid anaphase (Muscat et al., 2015; Fig. 1 A), these spindles instead appeared to have “closed poles,” with the microtubule channels blocked at the ends (Fig. 1 B and Fig. 2, A, B, and E). Because this microtubule density resembled the cupping shape of the kinetochores, we hypothesized that kinetochores might be making inappropriate attachments to microtubules,

enabling this extra accumulation. Therefore, we tested whether kinetochore disassembly was delayed under error conditions by examining the outer kinetochore component KNL-3, which normally cups the chromosome ends before anaphase and is removed from chromosomes by mid anaphase (Monen et al., 2005; Dumont et al., 2010). Notably, when we induced a ring disassembly delay, KNL-3 persisted on chromosomes (Figs. 3 C and S2 A). This finding reveals that kinetochore disassembly is also a regulated process that can be delayed in the presence of meiotic errors and illustrates that kinetochores may not have to be completely removed in order for chromosomes to segregate.

#### The response to errors requires the kinetochore but not components of the SAC

Next, we wanted to investigate how errors are detected in this unique form of cell division. Because univalents lack ring complexes (Muscat et al., 2015) but still elicit an error response

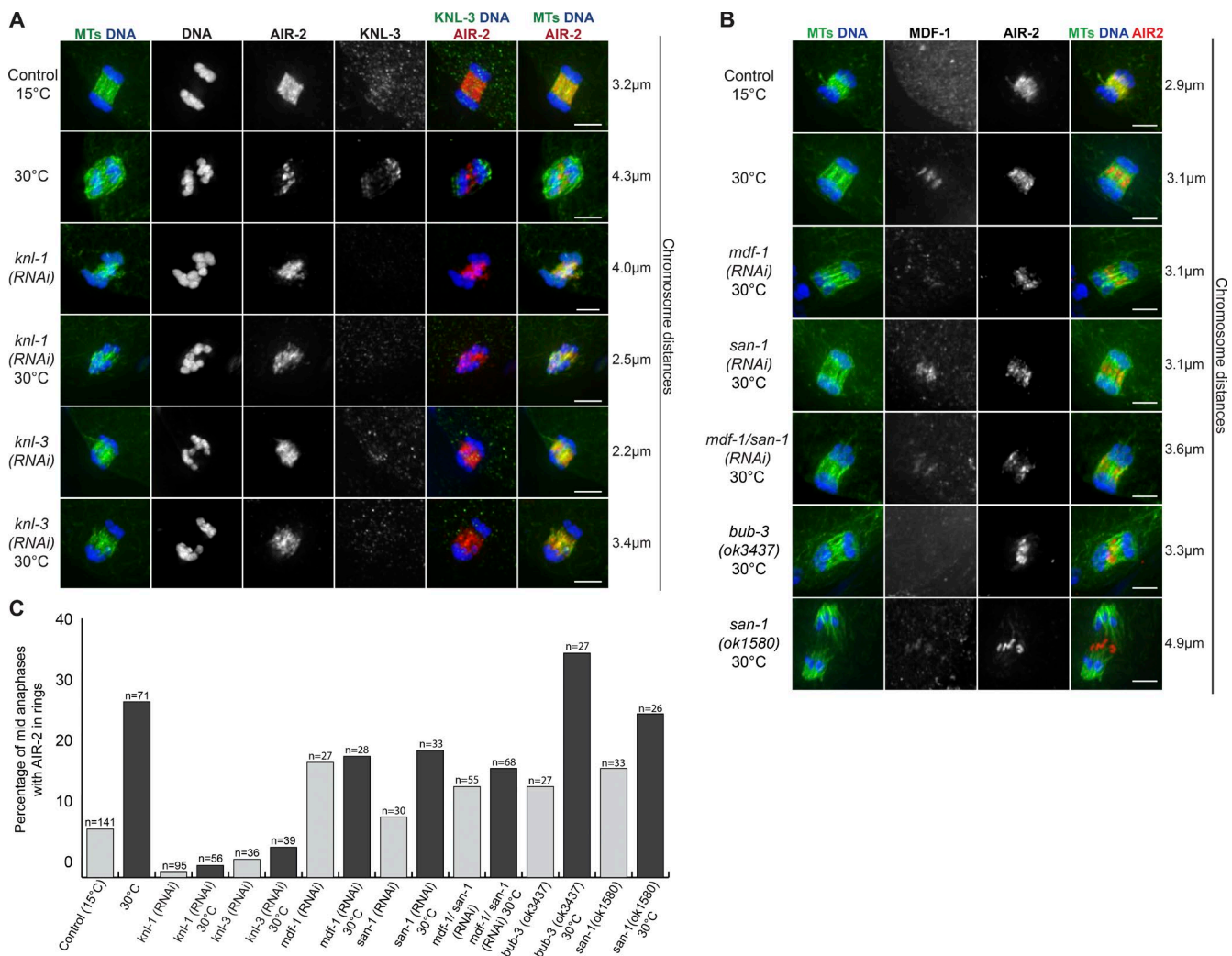


**Figure 4. The response to errors requires the kinetochore, but not components of the SAC.** (A) Mid anaphase spindles stained for DNA (blue), tubulin (green, columns 1 and 6), KNL-3 (green, column 5), and AIR-2 (red). Neither *knl-1(RNAi)* nor *knl-3(RNAi)* causes a ring disassembly delay. At 30°C, AIR-2 does not remain in rings after partial depletion of KNL-1 and KNL-3. Images were not restricted to the mid anaphase cutoff of  $\geq 2.5 \mu\text{m}$  to illustrate that AIR-2 relocates in early anaphase as well. (B) Mid anaphase spindles stained for DNA (blue), tubulin (green), AIR-2 (red), and MDF-1. AIR-2 remains in rings after 30°C treatment in worms depleted of MDF-1, SAN-1, and MDF-1/SAN-1 and in *bub-3* and *san-1* mutant strains. (C) Quantification of mid anaphase spindles with AIR-2 in rings for the kinetochore and SAC depletions at 15°C and 30°C. Includes MII spindles with chromosome distances  $\geq 2.5 \mu\text{m}$ . Note that depletion of SAC components alone (15°C) increased the percentage of spindles with AIR-2 in rings. In the case of MDF-1, this percentage did not increase significantly when combined with a 30°C treatment, suggesting that although MDF-1 does not appear to be absolutely required for an error response, its depletion may affect the magnitude of the response. Bars, 2.5  $\mu\text{m}$ .

(Fig. 1, B and C), it is unlikely that the ring complex itself acts as a sensor. Alternatively, in mitosis, errors are detected via end-on kinetochore attachments that generate tension across the chromosome. Although end-on attachments have not been observed in *C. elegans* oocytes, the holocentric kinetochores cup the ends of the bivalents before anaphase, placing them in a location where they could mediate side attachments to the lateral bundles. Moreover, kinetochore proteins coat the surfaces of univalents (Muscat et al., 2015), so they could theoretically participate in error sensing in those mutants as well.

To determine whether the kinetochore is required for the response to meiotic errors, we partially depleted outer kinetochore components KNL-1 and KNL-3 and assessed whether ring disassembly could be delayed in anaphase. These depletions caused metaphase defects, with bivalents misaligned within the lateral microtubule bundles (Fig. S2 B), and the spindles had lagging chromosomes in anaphase (Fig. 4 A), as previously

reported (Dumont et al., 2010). However, despite these errors, we did not observe a delay in AIR-2 relocation to the spindle or in ring disassembly (Fig. 4, A and C; and Fig. S2 C). Instead, depleting these kinetochore components prevented a ring disassembly delay, even under error conditions that would normally elicit this response (Fig. 4, A and C; and Fig. S2 C). These data therefore demonstrate that the kinetochore is required for delaying ring disassembly in response to errors; in this context, the kinetochores could play a role in sensing the errors or, alternatively, because they persist in the error conditions, they could be required for transducing the error signal.

This requirement for the kinetochore raises the possibility that the anaphase delays we observe are mediated by the SAC because that mechanism also relies on kinetochore function. Although we do not observe a metaphase arrest in response to errors, *C. elegans* embryos have been shown to have a weak SAC response (Encalada et al., 2005; Essex et al., 2009; Galli

and Morgan, 2016), so it is possible that the anaphase delays we observe could reflect a mild SAC response. To test this hypothesis, we inhibited SAC components and scored AIR-2 and ring anaphase behavior, with and without inducing an additional stress; for this analysis, we singly and doubly depleted *mdf-1* (Mad1) and *san-1* (Mad3) using RNAi and also assessed *san-1(ok1580)* and *bub-3(ok3437)* mutant strains. Unlike the kinetochore depletions, where nearly all error response was lost (Fig. 4, A and C), in the SAC mutant/depletion conditions, AIR-2 still persisted in rings after 30°C treatment. Notably, some SAC depletions induced an error response on their own (Fig. 4, B and C), suggesting that SAC components may play roles in oocyte meiosis but are likely not required for the observed anaphase delays.

As a part of this analysis, we also assessed MDF-1 (Mad1) localization, because this protein has been shown to transiently localize to the rings at anaphase onset (Moyle et al., 2014; Fig. S3 A), placing it in a location where it could potentially regulate AIR-2 relocalization to the microtubules and participate in the error response. However, we found that the MDF-1 localization pattern did not correlate with AIR-2 behavior. Although it was associated with the ring complexes just before AIR-2 relocalized to the microtubules, it also remained with the flattening rings well after AIR-2 removal (Fig. S3, A and B). MDF-1 persisted in rings during mid to late anaphase under error conditions, but because other components of the ring complex are also ring associated under these conditions (Figs. 2 E and S3 A), this behavior likely reflects a general stabilization of the ring structures and not a specific retention of MDF-1. Additionally, we found that in the *bub-3(ok3437)* mutant strain, MDF-1 no longer associated with the anaphase rings, demonstrating that BUB-3 is required for MDF-1 ring targeting but that this targeting is not required for the AIR-2 error response (Fig. 4 B). Therefore, although the intriguing MDF-1 localization pattern and its targeting by BUB-3 suggests that SAC components may have roles in oocyte meiosis, they do not appear to be necessary for the ring complex regulation we have uncovered, implying that in this mechanism, the kinetochore is required for the error response independent of MDF-1, SAN-1, and BUB-3.

### New insights into kinetochore-independent chromosome segregation

In summary, our studies have revealed that there is a regulatory mechanism that alters multiple aspects of anaphase progression in response to a variety of perturbations (Fig. 5), suggesting that errors can be detected in this system. We speculate that delaying ring disassembly and keeping the microtubule channels open could prevent the collapse of microtubule bundles around lagging chromosomes, allowing errors more time to resolve. This suggests that *C. elegans* oocytes use a mechanism that could serve to increase the fidelity of chromosome segregation, similar to checkpoints that operate in other cell types. However, this regulation does not appear to elicit a strong metaphase arrest, as is seen in mutants of the anaphase-promoting complex (Golden et al., 2000; Davis et al., 2002), because anaphase progresses and cytokinesis occurs in all cases. This is reflected in our quantification, as we do not observe rings persisting in all anaphase spindles in any mutant condition. Although it is possible that not every error is detected, it is also likely that many of the spindles we observe are past the point of delay.

Although it is possible that the timing of cell cycle events may be altered in response to error, we hypothesize that this

mechanism instead primarily represents a shift in the progression and coordination of anaphase events. A recent study defined *C. elegans* meiotic anaphase as having two distinct phases: anaphase A and B (McNally et al., 2016). Chromosomes exhibit poleward movement during anaphase A, when microtubule channels are open in the center of the spindle, kinetochores are still present on the chromosomes but are beginning to disassemble, and ring complexes are still intact but AIR-2 is beginning to relocalize. Then, in anaphase B, spindle elongation occurs to further separate chromosomes; at this stage the chromosomes have moved to the ends of the microtubule channels, the rings are disassembling, and the kinetochores are gone. Under normal conditions, anaphase A and B appear to be sequential mechanisms, with chromosome-to-pole movement preceding spindle elongation (McNally et al., 2016). In contrast, we speculate that under error conditions, maintaining ring complexes, kinetochores, and open microtubules channels could represent an extension of anaphase A mechanisms, keeping them active as the spindle elongates to facilitate chromosome segregation (Fig. 5). Our results therefore demonstrate that it is not essential to completely turn off the anaphase A mechanisms for anaphase B to proceed, implying that anaphase B spindle elongation can occur in the context of the anaphase A type of spindle organization, with open microtubule channels in the center of the spindle and lateral associations on the sides of chromosomes.

Another interesting aspect of our findings is that the delay in kinetochore removal led to extra microtubule density at the ends of the chromosomes in anaphase, suggesting that if kinetochores are not removed, the ends of the chromosomes become competent for microtubule association at this stage. This finding raises the intriguing possibility that kinetochores may form transient functional attachments that participate in the early stages of chromosome segregation; if this were the case, it could represent another mechanism that is retained under error conditions that could help promote chromosome segregation. However, because previous work demonstrated that chromosomes segregate at normal rates after KNL-1 depletion (even during anaphase A, when kinetochores would have been present on chromosomes; Dumont et al., 2010), even if these transient attachments form, they are unlikely to make a major contribution to chromosome segregation. Regardless of whether these extra microtubules are force generating, the fact that they appear to “block” the ends of the microtubule channels reveals a potential reason why kinetochores usually disassemble by mid anaphase; this could serve to clear a path so that the chromosomes can move past the poles.

Our finding that kinetochore disassembly is delayed under error conditions also reveals that although this form of chromosome segregation is usually kinetochore independent, kinetochore removal does not appear to be absolutely required for chromosome separation. This is an important finding, because a recent study proposed that kinetochores must be removed in order for chromosome segregation to occur (Hattersley et al., 2016). This hypothesis was based on the analysis of mutants where targeting of a phosphatase (GSP-2/PP1) to chromosomes was prevented; under these conditions, kinetochores did not disassemble and chromosomes did not segregate, but segregation was rescued when kinetochore components were also depleted. Given our finding that kinetochores are required for an error response, an alternate possibility to explain these data is that PP1 regulates aspects of anaphase progression as part of the mechanism we have described. If this were the case, kinetochore depletion would enable anaphase to proceed in mutants lacking

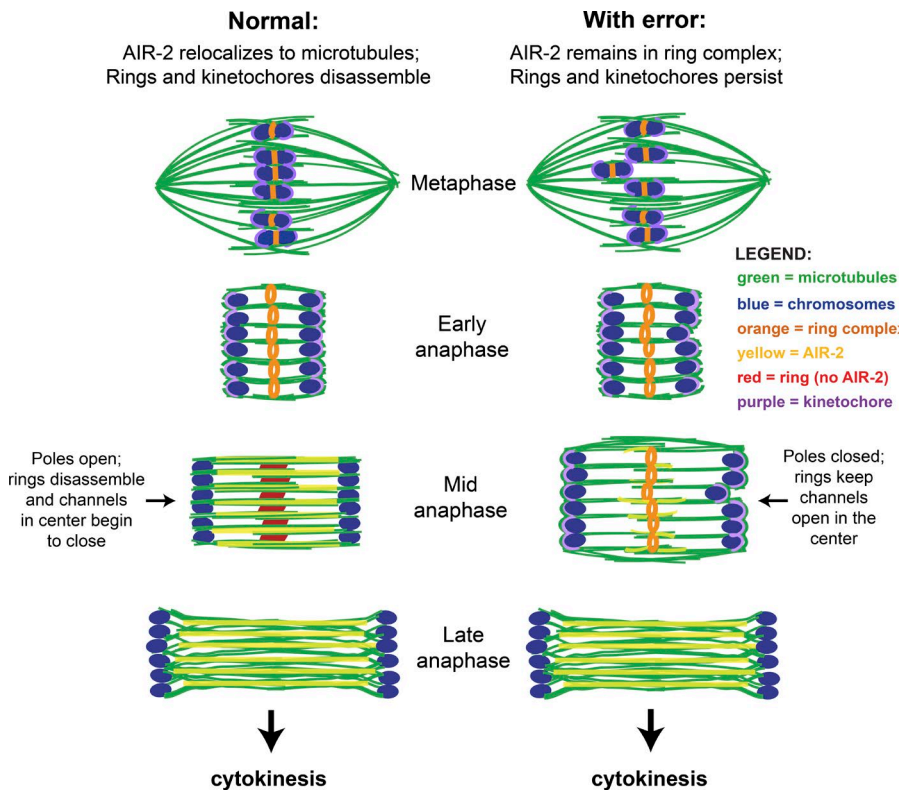


**Figure 5. Model for kinetochore and AIR-2/Aurora B-mediated anaphase regulation.** Model depicting DNA (blue), microtubules (green), the ring complexes with AIR-2 (orange), AIR-2 (yellow), the ring complexes without AIR-2 (red), and kinetochores (purple). In normal meiosis (left), kinetochores are removed from chromosomes, AIR-2 relocates to the microtubules, and the ring complexes begin to disassemble by mid anaphase. Under many types of perturbations (a congression defect is depicted on the right), AIR-2 remains with the rings throughout mid anaphase, keeping the microtubule channels open. Chromosomes continue segregating, despite retention of kinetochores on chromosomes. By late anaphase, AIR-2 relocates to the microtubules and cytokinesis occurs.

PP1 targeting, because under these conditions, the oocytes would bypass error detection. Therefore, future studies testing this possibility may shed light on the molecular mechanisms of ring and kinetochore disassembly.

Some important questions that arise from our discovery are when and how oocytes monitor and sense errors and what types of errors are detected. Because errors late in anaphase do not appear to be detected by this mechanism, our data point to detection occurring in either metaphase or very early anaphase. Intriguingly, it was recently shown that just before chromosome segregation, when the spindle shrinks and the poles come into close proximity with the kinetochores, the chromosomes and kinetochores appear to transiently stretch (McNally et al., 2016). This finding suggests that a tension-sensing mechanism acting at the metaphase to anaphase transition could monitor proper chromosome alignment; under this scenario, proper tension across the chromosome would promote AIR-2/Aurora B relocation to the microtubules. In this mechanism, tension could be generated using side attachments to the lateral bundles, mediated by kinetochore proteins cupping the bivalent ends or through transient end-on kinetochore attachments made when the spindle shrinks. In the latter situation, these transient attachments would be quickly lost as the kinetochores disassemble under normal conditions, but under the error conditions where kinetochores persist, they could be retained. Importantly, because neither of these potential mechanisms relies on canonical tension-generating end-on attachments that are in place before anaphase onset, our studies have revealed a new strategy for error detection during cell division. Future studies building on this work will shed light on how chromosomes are accurately segregated during this important specialized cell division.

## Materials and methods

### Strains

The quantification of control spindles includes both EU1067 and N2 (Bristol) (Figs. 1, S1, 2, and 4). For RNAi experiments, “control” refers to the RNAi vector control in EU1067 worms. The following strains were used in this study: N2; EU1067, *unc-119(ed3)* *ruls32*[*unc-119(+)* *pie-1*<sup>Promoter</sup>::GFP::H2B] III; *ruls57*[*unc-119(+)* *pie-1*<sup>Promoter</sup>::GFP::tubulin]; CA324, *zim-1*(*tm1813*) IV; FM13, *mei-2*(*ct98*) I; *ruls57*[*pAZ147*:*pie-1*<sup>Promoter</sup>::tubulin::GFP::unc-119(+)]; *itls37*[*unc-119(+)* *pie-1*<sup>Promoter</sup>::*mcCherry*::H2B]; *him-8*(*e1489*) IV; CA151, *him-8*(*me4*) IV; SMW6, strain EU1067 crossed with strain CA151 resulting in *unc-119(ed3)* *ruls32*[*unc-119(+)* *pie-1*<sup>Promoter</sup>::GFP::H2B] III; *ruls57*[*unc-119(+)* *pie-1*<sup>Promoter</sup>::GFP::tubulin]; *him-8*(*me4*) IV; VC2773, *bub-3*(*ok3437*) II; and RB1391, *san-1*(*ok1580*) I.

### RNAi

From a feeding library (Fraser et al., 2000; Kamath et al., 2003), individual RNAi clones were picked and grown overnight at 37°C in LB with 100 µg/ml ampicillin. Overnight cultures were spun down and plated on nematode growth media plates containing 100 µg/ml ampicillin and 1 mM IPTG. Plates were dried overnight. Worm strains were synchronized by bleaching gravid adults and hatching overnight without food. For full RNAi (*klp-19*, *capg-1*, *ani-1*, *aspn-1*, *mdf-1*, *san-1*, and all double depletions), L1s were then plated on RNAi plates and grown to adulthood at 15° for 4–5 d. When full RNAi prevented proper germline formation, partial RNAi was performed. For these depletions, worms were grown until the L2 (*knl-1* and *knl-3*) or L3 (*cyk-4*, *zen-4*) stage on regular nematode growth media OP50 plates and then transferred to the RNAi plate 48–72 h before preparing for immunofluorescence (Table 1).

### Immunofluorescence and antibodies

Immunofluorescence was performed as previously described (Oegema et al., 2001). In brief, worms were picked into a drop of M9 buffer and cut onto poly-L-lysine slides (Electron Microscopy Sciences) to release embryos. Slides were frozen in liquid nitrogen for 10 min, and then the coverslip was quickly removed with a razor blade. Embryos were fixed for 40–45 min in –20°C methanol, rehydrated in PBS, and blocked in AbDil (PBS plus 4% BSA, 0.1% Triton X-100, and 0.02% Na-Azide) at room temperature. Primary antibodies were diluted in AbDil and incubated overnight at 4°C. Secondary antibodies were diluted in AbDil and incubated for 1 h at room temperature. Hoechst 33342 (Invitrogen) was diluted 1:1,000 in PBST (PBS + 0.1% Triton X-100) and incubated for 10–15 min at room temperature. Slides were washed with PBST between antibody incubations and mounted in 0.5% p-phenylenediamine in 90% glycerol, 20 mM Tris, pH 8.8.

The following antibodies were used: rabbit anti–AIR-2 (1:1,000; gift from J. Schumacher, University of Pittsburgh, Pittsburgh, PA), rabbit anti–SEP-1 (1:350; gift from A. Golden, National Institutes of Health, National Institute of Diabetes and Digestive and Kidney Diseases, Bethesda, MD), rabbit anti–KNL-3 (1:3,800, gift from A. Desai, Ludwig Institute for Cancer Research, University of California, San Diego, CA), rabbit anti–MDF-1 (1:3,000; a gift from R. Kitagawa, Nationwide Children’s Hospital, Columbus, OH), mouse anti–MPM-2 (1:500; catalog number 05-368; EMD Millipore), and mouse anti– $\alpha$ -tubulin FITC (1:500; catalog number F2168; Sigma-Aldrich). Rat anti–AIR-2 was generated by Covance using the C-terminal peptide sequence KIRAEKQQKIEKEASLRNH (synthesized by the Peptide Synthesis Core Facility at Northwestern University) and then affinity purified and used at 1:1,000. Alexa Fluor 555– and 647-conjugated secondary antibodies (Invitrogen) were used at 1:500.

### Microscopy

All imaging was performed on a DeltaVision Core deconvolution microscope (Applied Precision Ltd.) with a Photometrics CoolSnap HQ2 camera using an Olympus 100 $\times$  oil objective (NA = 1.4). This microscope is housed in the Northwestern Biological Imaging Facility supported by the Northwestern University Office for Research. Slides were imaged at room temperature and image stacks were obtained at 0.2  $\mu$ m z-steps and deconvolved (ratio method, 15 cycles) using SoftWoRx (Applied Precision Ltd.). All images in this study were displayed as full maximum-intensity projections of data stacks encompassing the entire spindle structure unless otherwise noted.

### Image analysis and quantification

Imaris 3D Imaging Software (Bitplane) was used for chromosome distance and spindle width measurements. To calculate chromosome distances, the “Surfaces” tool was first used to determine the volume of

each grouping of separating chromosomes and then to assign the center of the volume for each set. The distance between these two center points was then measured as the chromosome segregation distance. For some conditions with severe chromosome segregation defects (e.g., the *zim-1* mutant or *centralspindlin* RNAi in MII), we could not accurately determine chromosome distance measurements for all spindles, because it was difficult to assign the chromosomes to two distinct groups. Therefore, these spindles were excluded from our analysis. Note that this may result in an underrepresentation of the percentage of spindles with AIR-2 in rings (data presented in Figs. 1 and 2) for some of the mutant conditions, because AIR-2 was often ring associated in these severely defective spindles. For spindle width measurements, images were viewed in the slice gallery, and a line was drawn across the width of the microtubule signal at the center of the spindle. This was done for three z-slices within each spindle, and the line lengths were averaged to obtain a spindle width measurement.

### Statistical methods

For spindle width measurements, the mean spindle widths for a given condition were compared with the control spindle widths using a two-tailed *t* test, resulting in a *p*-value of <0.001 for all three of the error-condition groups in which AIR-2 remained in rings. Data distribution was assumed to be normal, but this was not formally tested.

### Temperature experiments

EU1067 worms were picked into a drop of M9 preincubated at specific temperatures (4°C, 25°C, or 30°C), incubated for 4–5 min at the corresponding temperature, and prepared for immunofluorescence. The total time of incubation in M9 at a given temperature was ~10–15 min because of the picking and cutting steps. Note that this assay is also sensitive to the temperature of the room, as we have noticed a moderate increase in the number of control spindles with AIR-2 remaining in rings on days where the ambient temperature is higher. To ensure that this day-to-day variation did not significantly affect our conclusions, we controlled for temperature as closely as we could, and we made sure that each of our quantified conditions incorporated slides generated on multiple days.

### Determining anaphase stages

We analyzed 246 anaphase spindles, noting whether AIR-2 was relocalized across the microtubules or concentrated in rings (colocalized with another ring marker and within open microtubule channels). We then measured the chromosome segregation distance for all anaphase spindles and looked for the chromosome distance at which AIR-2 had relocalized to the microtubules in most spindles (Fig. S1). The 246 spindles analyzed includes both anaphase I and II spindles, as well as both N2 worms and EU1067, as the trends for chromosome

Table 1. Oligos used to create clones for feeding RNAi (Ahringer library)

Gene	Forward primer sequence (5'-3')	Reverse primer sequence (5'-3')
<i>klp-19</i>	CATAGCGAAGCGTGTGAGA	ATTGTGCGTGAACCTGACG
<i>capg-1</i>	TTGTAACCATTTCATGGCGA	CATGCCACCAACAGATCAACC
<i>aspn-1</i>	GCTTCAAGAACTACGACGCC	TGGGTGTTCCAACGGATAAT
<i>mdf-1</i>	CACGAGCGATTTCTCTTCC	TCTTCGAGTTGTTGGTG
<i>san-1</i>	AACGAAACAATGATGACGCA	TTTCGATGTGAGCATGAAGC
<i>ani-1</i>	CATGTTCACTGACAACCTGGGATA	CAAACCTCAATGGAGAGGACAATC
<i>knl-1</i>	GAAGCACTGAACACGTCCAA	ATTGTAGGCCCTGATGCAAGG
<i>knl-3</i>	TTTCGCCAGAAATTCTATCC	GCTCATCATCAGCAGTTCCA
<i>cyk-4</i>	TGGTTTGTCTGGTGTGTTGA	ACGGTTTCAAGCATTTCAT
<i>zen-4</i>	GGAAAATGATGGACAAGCTACTG	TCTTGAAATTCTGAACGAACCAT

distance and AIR-2 behavior were indistinguishable between these groups. We defined 2.5  $\mu$ m as roughly the transition from early to mid anaphase, the segregation distance at which AIR-2 should be relocalized in most wild-type spindles. All images labeled as mid anaphase, as well as all spindles quantified in Figs. 1 C, 2 D, 4 C, and S2, have a chromosome distance of at least 2.5  $\mu$ m. The spindle lengths at late anaphase were variable, so rather than using a specific chromosome distance, this stage was defined by the microtubules being severely collapsed and the chromosomes being significantly past the poles. Late anaphase spindles were excluded from all quantifications in Figs. 1 C, 2 D, 4 C, and S2.

### Online supplemental material

Fig. S1 shows the quantification of AIR-2 behavior in anaphase at given chromosome segregation distances. Fig. S2 shows other error conditions tested for kinetochore persistence, chromosome misalignment in metaphase in KNL-1 or KNL-3 depleted spindles, and other error conditions quantified for kinetochore dependence. Fig. S3 shows MDF-1 localization from metaphase through late anaphase and its delocalization in the *bub-3* mutant strain. Videos 1 and 2 show an anaphase spindle after *capg-1(RNAi)* with delayed AIR-2 relocalization to highlight that microtubule channels in the center of the spindle remain open.

### Acknowledgments

We thank members of the Wignall laboratory for support; Needhi Bhalla, Carissa Heath, Tim Mullen, Keila Torre-Santiago, and Ian Wolff for critical reading of the manuscript; and Arshad Desai, Andy Golden, Risa Kitagawa, and Jill Schumacher for reagents. Some strains were provided by the *Caenorhabditis Genetics Center*, which is funded by the National Institutes of Health Office of Research Infrastructure Programs.

This work was supported by a National Science Foundation Graduate Research Fellowship grant DGE-1324585, the Molecular Biophysics Training Program at Northwestern University (to A.C. Davis-Roca), and a March of Dimes Basil O'Connor Award and Damon Runyon-Rachleff Innovation Award (to S.M. Wignall).

The authors declare no competing financial interests.

Author contributions: S.M. Wignall, A.C. Davis-Roca, and C.C. Muscat were responsible for the experimental design. A.C. Davis-Roca and C.C. Muscat performed all of the experiments. A.C. Davis-Roca and S.M. Wignall wrote the manuscript with input from C.C. Muscat.

Submitted: 11 August 2016

Revised: 13 December 2016

Accepted: 14 February 2017

### References

Brenner, S. 1974. The genetics of *Caenorhabditis elegans*. *Genetics*. 77:71–94.

Cheerambathur, D.K., and A. Desai. 2014. Linked in: Formation and regulation of microtubule attachments during chromosome segregation. *Curr. Opin. Cell Biol.* 26:113–122. <http://dx.doi.org/10.1016/j.ceb.2013.12.005>

Collette, K.S., E.L. Petty, N. Golenberg, J.N. Bembeneck, and G. Csankovszki. 2011. Different roles for Aurora B in condensin targeting during mitosis and meiosis. *J. Cell Sci.* 124:3684–3694. <http://dx.doi.org/10.1242/jcs.088336>

Connolly, A.A., V. Osterberg, S. Christensen, M. Price, C. Lu, K. Chicas-Cruz, S. Lockery, P.E. Mains, and B. Bowerman. 2014. *Caenorhabditis elegans* oocyte meiotic spindle pole assembly requires microtubule severing and the calponin homology domain protein ASPM-1. *Mol. Biol. Cell.* 25:1298–1311. <http://dx.doi.org/10.1091/mbc.E13-11-0687>

Connolly, A.A., K. Sugioka, C.H. Chuang, J.B. Lowry, and B. Bowerman. 2015. KLP-7 acts through the Ndc80 complex to limit pole number in *C. elegans* oocyte meiotic spindle assembly. *J. Cell Biol.* 210:917–932. <http://dx.doi.org/10.1083/jcb.201412010>

Davis, E.S., L. Wille, B.A. Chestnut, P.L. Sadler, D.C. Shakes, and A. Golden. 2002. Multiple subunits of the *Caenorhabditis elegans* anaphase-promoting complex are required for chromosome segregation during meiosis I. *Genetics*. 160:805–813.

Dumont, J., K. Oegema, and A. Desai. 2010. A kinetochore-independent mechanism drives anaphase chromosome separation during acentrosomal meiosis. *Nat. Cell Biol.* 12:894–901. <http://dx.doi.org/10.1038/ncb2093>

Encalada, S.E., J. Willis, R. Lyczak, and B. Bowerman. 2005. A spindle checkpoint functions during mitosis in the early *Caenorhabditis elegans* embryo. *Mol. Biol. Cell.* 16:1056–1070. <http://dx.doi.org/10.1091/mbc.E04-08-0712>

Essex, A., A. Dammermann, L. Lewellyn, K. Oegema, and A. Desai. 2009. Systematic analysis in *Caenorhabditis elegans* reveals that the spindle checkpoint is composed of two largely independent branches. *Mol. Biol. Cell.* 20:1252–1267. <http://dx.doi.org/10.1091/mbc.E08-10-1047>

Etemad, B., and G.J. Kops. 2016. Attachment issues: kinetochore transformations and spindle checkpoint silencing. *Curr. Opin. Cell Biol.* 39:101–108. <http://dx.doi.org/10.1016/j.ceb.2016.02.016>

Fraser, A.G., R.S. Kamath, P. Zipperlen, M. Martinez-Campos, M. Sohrmann, and J. Ahringer. 2000. Functional genomic analysis of *C. elegans* chromosome I by systematic RNA interference. *Nature*. 408:325–330. <http://dx.doi.org/10.1038/35042517>

Galli, M., and D.O. Morgan. 2016. Cell size determines the strength of the spindle assembly checkpoint during embryonic development. *Dev. Cell.* 36:344–352. <http://dx.doi.org/10.1016/j.devcel.2016.01.003>

Golden, A., P.L. Sadler, M.R. Wallenfang, J.M. Schumacher, D.R. Hamill, G. Bates, B. Bowerman, G. Seydoux, and D.C. Shakes. 2000. Metaphase to anaphase (mat) transition-defective mutants in *Caenorhabditis elegans*. *J. Cell Biol.* 151:1469–1482. <http://dx.doi.org/10.1083/jcb.151.7.1469>

Han, X., K. Adames, E.M. Sykes, and M. Srayko. 2015. The KLP-7 residue S546 is a putative aurora kinase site required for microtubule regulation at the centrosome in *C. elegans*. *PLoS One*. 10:e0132593. <http://dx.doi.org/10.1371/journal.pone.0132593>

Hattersley, N., D. Cheerambathur, M. Moyle, M. Stefanutti, A. Richardson, K.Y. Lee, J. Dumont, K. Oegema, and A. Desai. 2016. A nucleoporin docks protein phosphatase 1 to direct meiotic chromosome segregation and nuclear assembly. *Dev. Cell.* 38:463–477. <http://dx.doi.org/10.1016/j.devcel.2016.08.006>

Hirsh, D., D. Oppenheim, and M. Klass. 1976. Development of the reproductive system of *Caenorhabditis elegans*. *Dev. Biol.* 49:200–219. [http://dx.doi.org/10.1016/0012-1606\(76\)90267-0](http://dx.doi.org/10.1016/0012-1606(76)90267-0)

Jantsch-Plunger, V., P. Gönczy, A. Romano, H. Schnabel, D. Hamill, R. Schnabel, A.A. Hyman, and M. Glotzer. 2000. CYK-4: A Rho family gtpase activating protein (GAP) required for central spindle formation and cytokinesis. *J. Cell Biol.* 149:1391–1404. <http://dx.doi.org/10.1083/jcb.149.7.1391>

Kamath, R.S., A.G. Fraser, Y. Dong, G. Poulin, R. Durbin, M. Gotta, A. Kanapin, N. Le Bot, S. Moreno, M. Sohrmann, et al. 2003. Systematic functional analysis of the *Caenorhabditis elegans* genome using RNAi. *Nature*. 421:231–237. <http://dx.doi.org/10.1038/nature01278>

Maddox, A.S., B. Habermann, A. Desai, and K. Oegema. 2005. Distinct roles for two *C. elegans* anillin in the gonad and early embryo. *Development*. 132:2837–2848. <http://dx.doi.org/10.1242/dev.01828>

McNally, K., A. Audhya, K. Oegema, and F.J. McNally. 2006. Katanin controls mitotic and meiotic spindle length. *J. Cell Biol.* 175:881–891. <http://dx.doi.org/10.1083/jcb.200608117>

McNally, K.P., M.T. Panzica, T. Kim, D.B. Cortes, and F.J. McNally. 2016. A novel chromosome segregation mechanism during female meiosis. *Mol. Biol. Cell.* 27:2576–2589. <http://dx.doi.org/10.1091/mbc.E16-05-0331>

Monen, J., P.S. Maddox, F. Hyndman, K. Oegema, and A. Desai. 2005. Differential role of CENP-A in the segregation of holocentric *C. elegans* chromosomes during meiosis and mitosis. *Nat. Cell Biol.* 7:1248–1255. <http://dx.doi.org/10.1038/ncb1331>

Moyle, M.W., T. Kim, N. Hattersley, J. Espeut, D.K. Cheerambathur, K. Oegema, and A. Desai. 2014. A Bub1-Mad1 interaction targets the Mad1-Mad2 complex to unattached kinetochores to initiate the spindle checkpoint. *J. Cell Biol.* 204:647–657. <http://dx.doi.org/10.1083/jcb.201311015>

Muscat, C.C., K.M. Torre-Santiago, M.V. Tran, J.A. Powers, and S.M. Wignall. 2015. Kinetochore-independent chromosome segregation driven by lateral microtubule bundles. *eLife*. 4:e06462. <http://dx.doi.org/10.7554/eLife.06462>

Oegema, K., A. Desai, S. Rybina, M. Kirkham, and A.A. Hyman. 2001. Functional analysis of kinetochore assembly in *Caenorhabditis elegans*. *J. Cell Biol.* 153:1209–1226. <http://dx.doi.org/10.1083/jcb.153.6.1209>

Phillips, C.M., and A.F. Dernburg. 2006. A family of zinc-finger proteins is required for chromosome-specific pairing and synapsis during meiosis in *C. elegans*. *Dev. Cell.* 11:817–829. <http://dx.doi.org/10.1016/j.devcel.2006.09.020>

Phillips, C.M., C. Wong, N. Bhalla, P.M. Carlton, P. Weiser, P.M. Meneely, and A.F. Dernburg. 2005. HIM-8 binds to the X chromosome pairing center and mediates chromosome-specific meiotic synapsis. *Cell.* 123:1051–1063. <http://dx.doi.org/10.1016/j.cell.2005.09.035>

Raich, W.B., A.N. Moran, J.H. Rothman, and J. Hardin. 1998. Cytokinesis and midzone microtubule organization in *Caenorhabditis elegans* require the kinesin-like protein ZEN-4. *Mol. Biol. Cell.* 9:2037–2049. <http://dx.doi.org/10.1091/mbc.9.8.2037>

Romano, A., A. Guse, I. Krascenitcova, H. Schnabel, R. Schnabel, and M. Glotzer. 2003. CSC-1: a subunit of the Aurora B kinase complex that binds to the survivin-like protein BIR-1 and the incenp-like protein ICP-1. *J. Cell Biol.* 161:229–236. <http://dx.doi.org/10.1083/jcb.200207117>

Schumacher, J.M., A. Golden, and P.J. Donovan. 1998. AIR-2: An Aurora Ipl1-related protein kinase associated with chromosomes and midbody microtubules is required for polar body extrusion and cytokinesis in *Caenorhabditis elegans* embryos. *J. Cell Biol.* 143:1635–1646. <http://dx.doi.org/10.1083/jcb.143.6.1635>

Speliotes, E.K., A. Uren, D. Vaux, and H.R. Horvitz. 2000. The survivin-like *C. elegans* BIR-1 protein acts with the Aurora-like kinase AIR-2 to affect chromosomes and the spindle midzone. *Mol. Cell.* 6:211–223. [http://dx.doi.org/10.1016/S1097-2765\(00\)00023-X](http://dx.doi.org/10.1016/S1097-2765(00)00023-X)

Strayko, M., D.W. Buster, O.A. Bazirgan, F.J. McNally, and P.E. Mains. 2000. MEI-1/MEI-2 katanin-like microtubule severing activity is required for *Caenorhabditis elegans* meiosis. *Genes Dev.* 14:1072–1084.

van der Voet, M., C.W. Berends, A. Perreault, T. Nguyen-Ngoc, P. Gönczy, M. Vidal, M. Boxem, and S. van den Heuvel. 2009. NuMA-related LIN-5, ASPM-1, calmodulin and dynein promote meiotic spindle rotation independently of cortical LIN-5/GPR/Galpha. *Nat. Cell Biol.* 11:269–277. <http://dx.doi.org/10.1038/ncb1834>

Wignall, S.M., and A.M. Villeneuve. 2009. Lateral microtubule bundles promote chromosome alignment during acentrosomal oocyte meiosis. *Nat. Cell Biol.* 11:839–844. <http://dx.doi.org/10.1038/ncb1891>